Diabetes Publish Ahead of Print, published online August 3, 2009

REDUCTIVE METABOLISM OF AGE PRECURSORS: A METABOLIC ROUTE FOR PREVENTING AGE ACCUMULATION IN CARDIOVASCULAR TISSUE

Shahid P. Baba, Oleg A. Barski, Yonis Ahmed, Timothy E. O'Toole, Daniel J. Conklin, Aruni Bhatnagar, and Sanjay Srivastava

Diabetes and Obesity Center, University of Louisville, Louisville, KY 40202

Short Running Title: AR and metabolism of AGE precursors

Address correspondence to:
Sanjay Srivastava, Ph.D.
Email: sanjay@louisville.edu

Additional information for this article can be found in an online appendix at
http://diabetes.diabetesjournals.org

Submitted 12 March 2009 and accepted 18 Jul 2009.

Objective: To examine the role of aldo-keto reductases (AKRs) in the cardiovascular metabolism of the precursors of advanced glycation end products (AGEs).

Research Design and Methods: Steady-state kinetic parameters of AKRs with AGE precursors were determined using recombinant proteins expressed in bacteria. Metabolism of methylglyoxal and AGE accumulation were studied in human umbilical vein endothelial cells (HUVECs), C57-wild-type, *akr1b3* (aldose reductase, AR)-null and cardiospecific *akr1b4* (rat AR) and *akr1b8*-(FR-1) transgenic mice. AGE accumulation and atherosclerotic lesions were studied 12 weeks after streptozotocin-treatment of C57, *akr1b3*-null, and *apoE*- and *akr1b3*-*apoE*-null mice.

Results: Higher levels of AGEs were generated in the cytosol than at the external surface of HUVECs cultured in high glucose, indicating that intracellular metabolism may be an important regulator of AGE accumulation and toxicity. *In vitro*, AKR 1A and 1B catalyzed the reduction of AGE precursors, whereas AKR1C, AKR6, and AKR7 were relatively ineffective. Highest catalytic efficiency was observed with AKR1B1. Acetol formation in methylglyoxal-treated HUVECs was prevented by the AR inhibitor sorbinil. Acetol was generated in hearts perfused with methylglyoxal and its formation was increased in *akr1b4*- or *akr1b8*-transgenic mice. Reduction of AGE precursors was diminished in hearts from *akr1b3*-null mice. Diabetic *akr1b3*-null mice accumulated more AGEs in the plasma and the heart than WT mice and deletion of *akr1b3* increased AGE accumulation and atherosclerotic lesion formation in *apoE*-null mice.

Conclusion: Aldose reductase-catalyzed reduction is an important pathway in the endothelial and cardiac metabolism of AGE precursors and it prevents AGE accumulation and atherosclerotic lesion formation.

[1]The abbreviations used are: AGE, advanced glycation end products, AR, aldose reductase; BBGC Bromobenzyl glutathione cyclopentyl diester, BSTFA, *N,O*-bis (trimethylsilyl) trifluoroacetamide with trimethylchlorosilane; CML carboxy methyl lysine; MALDI-TOF/MS, mass-assisted laser desorption ionization time of flight mass spectrometry; ESI/MS, electrospray ionization mass spectrometry; DTT, dithiothreitol; ECL, enhanced chemiluminescence; HG high glucose; HUVECs, human umbilical vein endothelial cells; IPG strips, immobilized pH gradient strips; KH buffer, Krebs-Henseleit buffer; MG methylglyoxal; $NaBH_3CN$ sodiumcyanoborohydride; NG normal glucose; PFBHA, O-(2,3,4,5,6 pentaflourobenzyl)-hydroxylamine hydrochloride; PVDF, polyvinyl difluoride; ROS, reactive oxygen species; SDS, sodium dodecyl sulfate; TCA, trichloroacetic acid.

Non-enzymatic glycation and oxidation of proteins and lipids results in the formation of advanced glycation end products (AGEs) (1;2). The AGEs are formed when α-dicarbonyl and oxoaldehydes react with amines (Maillard reaction). These reactions generate multiple products that lead to Amadori modified proteins or aminophospholipids. AGEs are generated normally as tissues age, but they are formed at an accelerated rate during diabetes (3;4). Excessive AGE formation has been linked to cross-linking of matrix molecules such as collagen, vitronectin, and laminin (3;5;6). In addition binding of AGEs to RAGE results in the activation of MAP kinases, NF-κB, and CREB (7;8). These events stimulate the production of reactive oxygen species (ROS), and lead ultimately to an increase in vascular permeability and inflammation. The pathological significance of such receptor-mediated events is underscored by studies showing that RAGE blockage suppresses accelerated atherosclerotic lesion formation in diabetic mice (9), decreases neointimal expansion (10), and restores diabetic deficits in wound healing (11). Pharmacological blockage or genetic deletion of RAGE has been shown also to decrease albuminuria and mesangial expansion/glomerulosclerosis in mouse models of type 1 diabetes (12). Taken together, these studies suggest that the AGEs are significant mediators of hyperglycemic injury.

In most tissues, AGEs are derived from products generated from the autooxidation of glucose and fructose. These include deoxyglucosone, methylglyoxal, and glyoxal (1;2). Methylglyoxal is generated non-enzymatically from the oxidation and spontaneous dismutation of intermediates in the glycolysis pathway or enzymatic oxidation reaction catalyzed by peroxidases, whereas other AGE precursors such as deoxyglucosone are generated from fructose or from non-enzymatic degradation of Amadori rearrangement compounds (13). Previous studies show that the AGE precursor methylglyoxal is metabolized and detoxified by the glyoxalase system consisting of glyoxalase-I and -II (14;15). Nevertheless, the participation of other enzymes in the metabolism of methylglyoxal and other AGE precursors remains unclear. *In vitro* studies show that members of the aldo-keto reductase (AKRs) superfamily catalyze methylglyoxal reduction (16;17), and, in bacteria, these enzymes participate in the conversion of methylglyoxal to acetol (18;19). Nevertheless, the *in vivo* role of AKRs in mammalian metabolism of AGE precursors has not been studied. Accordingly, we tested the efficacy of several AKRs in catalyzing the reduction of AGE precursors. Our results show that reduction catalyzed by aldose reductase (AR; AKR1B) is a significant metabolic fate of AGE precursors in endothelial cells and in the heart, and that this metabolism prevents AGE accumulation during diabetes and atherosclerosis.

RESEARCH DESIGN AND METHODS

See the online supplement available at http://diabetes.diabetesjournals.org.

RESULTS

High glucose-induced AGE formation: AGEs are generated from non-enzymatic processes both in the cytosol and at the external matrix. To examine AGE abundance in these compartments, HUVECs were cultured in media containing normal (5.5 mM) and high (30 mM) glucose for 7 days and AGE formation was measured. Western analysis of the total cell lysates using the anti-argpyrimidine antibody showed that cells cultured in high glucose accumulated more AGEs than those grown in normal medium (Fig. 1A). Upon 2D gel electrophoresis and MALDI-MS analysis, the major

immunopositive protein was identified to be HSP27 [Fig 1A, inset], indicating that intracellular proteins are most likely to participate in AGE formation. These observations are in agreement with the studies by Schalkwijk *et al.,* (20) showing that high glucose selectively increases argpyrimidine adduct formation (with HSP27) in endothelial cells. However, to examine the extent of formation of extracellular AGEs intact cells were stained with the anti-argpyrimidine antibody and cell fluorescence was measured by FACS. To measure intracellular AGEs, the cells were permeabilized and then treated with anti-argpyrimidine antibody. Although minimal fluorescence was detected in non-permeabilized cells [Fig. 1B (i ii)], permeabilization increased fluorescence in both normal and high glucose-treated cells [Fig. 1B (iii iv)]. Relative fluorescence was higher in cells cultured in high glucose than in normal glucose medium. These data indicate that high glucose promotes AGE formation, and that most AGEs are generated in intracellular proteins such as HSP27. It follows then that accumulation and toxicity of AGEs is likely to be regulated not only by processes that generate AGE forming species, but also by intracellular pathways that metabolize AGE precursors.

Relative efficacy of AKRs in AGE reduction: Although methylglyoxal and glyoxal are known to be metabolized by glyoxalases (14;15), the metabolism of other AGE precursors remain unknown. It is also unclear whether methylglyoxal and glyoxal are metabolized by pathways other than glyoxalases. Hence, we measured the catalytic efficiencies of the human AKRs (AKR1, AKR6 and AKR7 families), some of which have been shown to catalyze methylglyoxal reduction *in vitro* (16). For these experiments, the AKR coding sequences containing His-tag were expressed in *E. coli* and the proteins were purified on a Ni-affinity column. Using glyoxal or methylglyoxal as substrates, highest catalytic efficiency was observed with AKR1B1 (human aldose reductase; AR). For both AKR1B1 and AKR1B3 (mouse AR), methylglyoxal was a better substrate than glyoxal. AKR1A4 (aldehyde reductase) was also an efficient catalyst for methylglyoxal reduction, although its catalytic activity with glyoxal was much less than that of AKR1B1. Members of the AKR1C and AKR7A5 family displayed low catalytic efficiencies, due largely to their high K_m values (Table 1).

AKR1B1 was also efficient at catalyzing the reduction of furfural and hydroxymethylfurfural, which are the major AGE precursors found in food (21). Daily human consumption of hydroxymethylfurfural is about 50 mg/kg per day (22). Furfural was reduced by AKR1B1, AKR1B3 and AKR1B10 with a catalytic efficiency that was higher than glyoxal. In contrast, hydroxymethylfurfural was poorly reduced by any of the AKRs. AKR1B1 and AKR1B3 were also efficient with the AGE precursor 3-deoxyglucosone, which was reduced efficiently by AKR1A4 as well (Table 1). Collectively, these data indicate that AKR1B1 (AR) is the most efficient enzyme involved in the reduction of several naturally-occurring AGE precursors. The role of other AKRs, however, could not be discounted. Some of these enzymes displayed high k_{cat} values with the AGE precursors, and their contribution to AGE metabolism may depend upon their relative abundance in specific tissues and the presence of other pathways of subsidiary metabolism.

Reductive metabolism of AGE precursors: Given that our results indicated that AKRs catalyze the reduction of AGE precursors and that AGEs accumulate intracellularly, we tested whether in cells methylglyoxal undergoes reductive transformation. For this, HUVECs were incubated with methylglyoxal and their lysates were used to measure acetol formation.

Upon GC analysis, reagent methylglyoxal [(R_t = 13.1; Fig. 2A(i)] was well-separated from acetol [R_t = 7.5; Fig. 2A (ii)]. Mass analysis of acetol revealed characteristic fragments with *m/z* 326 and 285 [Fig. 2A (ii)]. Similar fragments were obtained with $^{13}C_3$-acetol (*m/z* 329 and 286) with expected shift in mass. Using the $^{13}C_3$-labeled internal standard, the abundance of acetol was measured from cells that were either left untreated or treated with the AKR1B inhibitors-sorbinil or tolrestat. Ions with *m/z* 285 and 326 were used to quantify the abundance of natural acetol. The concentration of these ions was calculated using m/z 286 and 329 ions of the ^{13}C-internal standard. In cells incubated with methylglyoxal, the average concentration of acetol was 6.2 ± 0.7 (n=4) nmoles/mg protein. Treatment with sorbinil or tolrestat led to a significant decrease in the intensity of these ions [Fig. 2A(iii)]. These results demonstrate that in HUVECs, AKR1B catalyzes the reduction of methylglyoxal to acetol.

To examine the role of AKR1B in regulating AGE formation, HUVECs were cultured in high glucose (30 mM) media and steady-state levels of the most abundant AGE protein [Fig. 2B] AGE-HSP27 was measured. As before, incubation with glucose increased the levels of anti-arpyrimidine reactive HSP27, but the abundance of AGE-HSP27 was increased further in cells treated with sorbinil. No changes in the total protein levels of HSP27 were observed. In addition to the anti-argpyrimidine antibody, which recognizes arginine adducts of methylglyoxal, we also examined the formation of adducts between glyoxal and lysine using the anti-CML antibody**.** Treatment with high glucose, however, did not increase anti-CML reactivity and this reactivity was not affected by sorbinil (data not shown), indicating that under the experimental conditions studied, arginine adducts were more abundant. Overall, these results indicated that in HUVECs inhibition of AKR1B (AR) increases the formation and accumulation of argpyrimidine containing HSP27.

***Role of AKR1B in methylglyoxal metabolism*:** To determine whether methylglyoxal is metabolized to acetol in the heart, WT and AKR1B4 (rat AR)-TG mouse hearts were continuously perfused with methylglyoxal, and the perfusate was collected. The expression of the transgene was driven by the α-myosin heavy chain promoter, leading to cardiomyocyte-restricted increase in gene expression, thus changes in methylglyoxal metabolism could be attributed to cardiomyocyte-specific metabolism. GC-MS analysis of the perfusate revealed clearly resolved ions with *m/z* 285 and 326, which were ascribed to acetol. The concentration of acetol in effluents of AR-TG hearts was significantly higher (45±4 pmoles/ml) than that collected from WT hearts (25±3 pmoles/ml; Fig. 3A), indicating that an increase in AR in the heart increases the metabolism of methylglyoxal to acetol.

Myocytes isolated from mouse hearts expressed AKR1B3 (AR), AKR1B8 (FR-1), but not AKR1A3 (Fig. 3B). To establish the contribution of these enzymes, reduction of methylglyoxal was measured in cardiac homogenates of WT, AKR1B4-TG and AKR1B8-TG hearts, with cardiomyocyte-restricted expression of the transgene. Significant rates of methylglyoxal reduction were observed in WT cardiac homogenates. Methylglyoxal reduction was inhibited by sorbinil, indicating that the reaction was catalyzed by AKR1B (Fig. 3C). That AKR1B reduces methylglyoxal in the heart is further supported by data showing a significant increase in reduction rates in hearts of AKR1B4 or AKR1B8-TG mice (Fig. 3C). In agreement with *in vitro* data (Table 1), the methylglyoxal reductase activity in AKR1B4-TG mice was 35% higher than methylglyoxal reductase activity in the AKR1B8-TG hearts, indicating that AKR1B1/3/4 is a better

methylglyoxal reductase than AKR1B8. Based on these observations, we conclude that aldose reductase (AKR1B1/3/4) plays a major role in the reductive metabolism of methylglyoxal; however, AKR1B8 can also catalyze methylglyoxal reduction.

Because the purified AKR1B proteins were found to catalyze the reduction of several different AGE precursors, we also measured the reduction of major AGE precursors in cardiac homogenates of WT and AKR1B3-null mice. Methylglyoxal and deoxyglucosone reductase activities [Fig.4A (ii, iii)] in WT mice were similar in magnitude to the DL-glyceraldehyde reductase activity in these hearts [Fig. 4A(i)], whereas, glyoxal reduction [Fig. 4A (iv)] was 2-fold lower than the DL-glyceraldehyde reductase activity. Reduction of AGE precursors was significantly inhibited by sorbinil in WT, but not in AKR1B3-null; consistent with the involvement of AKR1B3 in this reduction.

In addition to AKRs, glyoxalase I is also involved in the metabolism of methylglyoxal. To determine the relative contribution of the two enzymes to the overall methylglyoxal metabolism, we measured the expression and activity of glyoxalase I in cardiac homogenates of WT and *akr1b3*-null mice. Glyoxalase I protein was abundant in the heart and its abundance was not affected by deletion of the *akr1b3*-gene. Our kinetic measurements indicated that 100±8 nmoles/min/mg protein of S-D-lactoylglutathione (a product of glyoxalase I) were generated in the heart. S-D-lactoylglutathione formation was significantly inhibited by glyoxalase 1 inhibitor BBGC [Fig. 4B (i)], indicating that it is primarily derived from glyoxalase I. Approximately 3-4 nmoles/min/mg protein of *S*-glycolylglutathione were formed by glyoxalase I when glyoxal was used as substrate [Fig 4B (ii)]. The values of the kinetic parameter of glyoxalase I were similar to those reported by Allen *et. al* (23) . No glyoxalase I activity was observed with deoxyglucosone. Metabolism of methylglyoxal by glyoxalase I was approx 10-fold higher than the methylglyoxal reductase activity by AKR1B3 (10±2 nmoles acetol/min/mg protein; [Fig 4A (i)]. Formation of *S*-glycolylglutathione by glyoxalase I from glyoxal was, however, approximately same as the reduction of glyoxal by AKR1B3 [Fig 4A (iv)]. To assess the relative contribution of AR and glyoxalase I in the metabolism of AGE precursors in the heart, we performed simulation experiments using the steady-state kinetic parameters listed in *Supplemental Table 1*. These calculations suggest that at low concentrations (glyoxal 1-100 μM and methylglyoxal 1-20 μM) AR-catalyzed reduction accounts for ~85 % of glyoxal and ~40% of methylglyoxal metabolism, while glyoxalase I contributes to ~15% glyoxal and ~60% methylglyoxal metabolism. At higher concentrations the relative contribution of glyoxalase I increases as a function of substrate concentration. This analysis is in agreement with the kinetic model of methylglyoxal metabolism in yeast (24). Together, these analyses suggest that both AR and glyoxalase I play significant and non-redundant roles in the metabolism of AGE precursors.

Regulation of AGE formation by AKR1B3: To examine how AKR1B3 regulates AGE formation in diabetes, WT and *akr1b3*-null mice were made diabetic by injecting STZ. Control mice were treated with the vehicle alone. Induction of diabetes led to an increase in HbA1c levels from 5.4±1.1% to 7.9±1.1% after 8 weeks of diabetes (data not shown). The STZ-mice showed marked hyperglycemia and the levels of plasma glucose, when measured after 12 weeks, were slightly higher in the AR-null than WT mice (Supplemental Table 2). Detectable levels of multiple argpyrimidine-derived AGEs were present in murine plasma. Quantification of

clearly-resolved band at 27 kDa showed that the intensity of this band was higher in diabetic mice (Fig 5A) The intensity of this band was even greater in *akr1b3*-null diabetic mice, indicating that deletion of this gene increases the formation of 27 kDa argpyrimidine AGE in the plasma of diabetic mice. Similar changes were observed when AGE formation was detected using the anti-CML antibody. As shown in Fig. 5B, increased accumulation of CML AGEs (2-12 fold) p 27, p 40 and p100 kDa was detected in the plasma of diabetic and non-diabetic *akr1b3*–null mice. Overall, the *akr1b3*-null diabetic plasma showed a greater plasma AGE accumulation than plasma from WT mice. This data suggests that deletion of the *akr1b3* gene increases AGE accumulation in the plasma.

To evaluate changes in tissue levels, AGE formation was quantified in the hearts. In hearts of 20-week old *akr1b3*-null diabetic mice, AGEs of 20 and 40 kDa were detected by anti-argpyrimidine and anti- CML antibodies (Fig. 6 A B). Changes in AGE formation in the hearts of WT and *akr1b3*-null mice were similar to those observed in the plasma. Induction of diabetes was associated with greater AGE accumulation in WT hearts due largely to the increase in p20 and p40 AGE. In contrast, in hearts of diabetic *akr1b3*-null mice, higher accumulation of p20 and p40 AGEs was observed. In each case, 2-3- fold increase in the abundance of these AGEs was observed in *akr1b3*-null than in WT hearts (Fig. 6B). However, the intensity of some of the anti-AGE antibody positive bands was decreased in the diabetic AR-null mice. The reasons for this decrease are unclear, but it is unlikely to be due to non-specific reactivity of the antibody, in which case the intensity would remain the same. Because the 45 and 40 kDa proteins show reciprocal relationship, we speculate that the 45 and the 40 kDa proteins may be the same protein and that due to multiple AGE formation its apparent molecular weight shifts from 45 to 40 kDa. Further experiments are, however required to identify changes in individual bands. Nevertheless, overall these data support the view that AKR1B3 prevents AGE formation and that metabolism of AGE precursors by this enzyme prevents AGE accumulation.

To examine AGE localization, sections of the diabetic hearts were stained with the anti-argpyrimidine antibody. Low levels of positive reactivity with the antibody were observed in WT diabetic hearts. This staining was associated strongly with blood vessels, but the cardiac myocytes showed diffuse staining as well (Fig. 6C). Staining of both myocytes and blood vessel was 2-3-fold higher in the diabetic *akr1b3*-null than WT hearts (Fig. 6C). These results indicate that deletion of *akr1b3* increases cardiovascular AGE accumulation in diabetes.

To assess how AKR1B3 regulates AGE formation during atherosclerosis, we generated *akr1b3-apoE*- null mice. Diabetes was induced by STZ and lesion formation was examined 12 weeks after the induction of diabetes. The levels of blood glucose, cholesterol and triglycerides in *akr1b3-apoE*-null mice were similar to those in mice null in *apoE* alone (Supplemental Table 2). Image analysis of hematoxylin-eosin stained sections of innominate arteries showed that lesion sizes in the aorta of diabetic *akr1b3-apoE* null mice were 2-3-fold higher than diabetic *apoE*-null mice (Fig. 7A). These data support the notion that deletion of the *akr1b3* gene increases atherosclerotic lesion formation in *apoE*-null mice.

Increase in lesion formation in the *akr1b3-apoE*- null was accompanied by an increase in AGE accumulation. For quantifying AGE formation, lesions of comparable sizes were stained with 3 different anti-AGE antibodies. As shown in Fig. 7, low levels of positive staining was observed in *apoE*-null mice, however, the

extent of staining was 3-4-fold higher in the *akr1b3-apoE-* null mice. Lesions of the *akr1b3-apoE*-null mice showed increases in their reactivity to anti-argpyrimidine, anti-CML, and anti-3-deoxyglucosone-imidazolone antibodies.Anti-argpyrimidine positive immunostaining was more predominant in the endothelial layer and the highly proliferative areas of the lesions as well as smooth muscle cells (Fig 7B). Staining for CML was particularly localized to atherosclerotic plaques (Fig 7C), whereas the staining for 3-deoxyglucosone-imidazolone increased both in smooth muscle cells and endothelial layer. Intense staining was also observed in the adventitia (Fig. 7D). Collectively, these data indicate that in diabetic *apoE*-null mice, deletion of *akr1b3* increases the formation of several structurally different AGEs.

DISCUSSION

The major findings of this study are that AR (AKR1B1/3/4)-catalyzed reduction is a significant pathway for the cardiovascular metabolism of AGE precursors and that the reduction of AGE precursors by AR diminishes the AGE formation and accumulation. Our observations that AR reduces a variety of AGE precursors and that pharmacological inhibition or genetic deletion of the enzyme increases AGE accumulation both in cells exposed to high glucose and in diabetic mice provides direct evidence supporting the notion that AR prevents AGE accumulation *in vivo* by detoxifying AGE precursors. These findings provide a new view of the role of this enzyme in the development of secondary diabetic complications.

Formation and accumulation of AGEs has been linked to the development of several diabetic complications (1;25-27). The AGEs are formed by reactions of proteins with glucose-derived carbonyls and could be generated either inside cells or on the extracellular surface, leading to collagen crosslinking (3). Our results, however, show that most AGEs, at least during short-term hyperglycemia, are generated within cells, indicating that metabolism of AGE-precursors could affect AGE formation. Intracellular formation of AGEs suggests that their formation could be regulated by the metabolism of AGE precursors. Indeed the AGE precursors methylglyoxal and glyoxal have been shown to be metabolized by glyoxalases and overexpression of glyoxalase I prevents AGE formation in endothelial cells cultured in high glucose (14) . Nonetheless, the *in vivo* role of glyoxalase I in preventing AGE formation in diabetic animals has not been tested. Moreover, given the limited substrate specificity of glyoxalase I, it is not clear how AGE precursors other than methylglyoxal (e.g. deoxyglucosone, furfural, hydromethyfurfural) are metabolized. Therefore, we studied the AKRs superfamily. Many members of this family catalyze the reduction of keto-aldehydes (28). We found significant activity with AKR1A4, AKR1B1, AKR1B3, AKR1B7, and AKR1B8. No activity was observed with the AKR1C family. Even with AKRs, family-wide variations in catalytic activities were observed with different AGE precursors, indicating that these enzymes may have tissue-specific role such that in tissues in which they are expressed in highest abundance, they may be capable of metabolizing AGE precursors. Consistently high activity was, however, observed with AKR1B1/3 (AR); indicating that this enzyme is likely to play the most general and significant role in the reduction of AGE precursors.

Previous work shows that AR is a broad-specificity aldehyde reductase. It catalyzes the reduction of several endogenously generated aldehydes including glucose, products of lipid peroxidation such as HNE (28-32), as well as AGE precursors such as methylglyoxal (16;33). Over

expression of AR in kidney tubules decreases carbonyl content (34) and the deletion of the AR gene in *Saccharomyces cervisiae* enhances the accumulation of argpyrimidine adducts (24). Studies from our lab show that AR prevents ischemia–injury (35) and mediates ischemic preconditioning (36), indicating that the enzyme may be involved in removing reactive aldehydes. The results of the current study, however, establish, for the first time, the *in vivo* cardiovascular role of AR in the metabolism of methylglyoxal and other AGE precursors. Several lines of evidence indicate that AR is a significant route of methylglyoxal metabolism. These include data showing that (1) acetol is generated in hearts perfused with methylglyoxal; (2) in endothelial cells AR inhibition increases AGE formation; and (3) reduction of methylglyoxal is increased in AR-TG hearts and decreased in AR-null hearts. A significant, non-redundant role of AR in the metabolism of AGE precursors is also supported by the observation that higher AGE levels were detected in AR-null than in WT mice. In comparison with tissues of WT mice, AR-null mouse heart and plasma showed higher abundance of several AGEs that reacted with the anti-argpyrimidine, anti-CML antibodies, and anti-3 deoxyglucosone imidazolone antibodies. The difference between WT and AR-null mouse tissues was evident even in the absence of diabetes, indicating that AGEs are formed during normal metabolism and that AR metabolizes AGE precursors even under basal conditions.

A significant role of AR in preventing AGE accumulation, indicated by our data, is in contrast to the current view that the polyol pathway generates AGEs (8;37). In the polyol pathway glucose is reduced to sorbitol by AR and then sorbitol is converted to fructose by sorbitol dehydrogenase. In the lens, fructose-3-phosphate is then generated either from the phosphorylation of fructose by 3-phosphokinase or the reduction of sorbitol-3-phosphate (38). Fructose-3-phosphate then spontaneously breaks down into 3-deoxyglucosone (39), which generates CML or imidazolone adducts (37). In agreement with this view it has been shown that plasma levels of 3-deoxyglucosone are increased in erythrocytes of diabetics and inhibition of AR decreases the levels of CML adducts in the erythrocytes (37). Nonetheless, even in the lens, fructose-3-phosphate is not generated upon incubation with high glucose (only with high fructose) (40). In cardiovascular tissues, it is not clear whether the low levels of sorbitol dehydrogenase (41) are sufficient to support significant formation of fructose from glucose. Moreover, as shown in current study, AR directly catalyzes the reduction of 3-deoxyglucosone and in contrast to changes seen in erythrocytes (37), genetic deletion of AR increased the abundance of CML adducts in diabetic heart and 3-deoxyglucosone derived imidazolone adducts in atherosclerotic lesions of diabetic mice. This disagreement may be due to differences in the tissue-specific roles of the AR or sorbitol dehydrogenase expression, or metabolic conditions that either favor the removal or the production of deoxyglucosone and other AGEs by AR. Nonetheless, the observation that lack of AR permits greater accumulation of several structurally-diverse AGEs suggests that the role of this enzyme is more complex than previously thought, and that at least in cardiovascular tissues AR prevents metabolites of glucose from forming AGEs.

Our results also show that atherosclerotic lesion formation in *apoE*-null mice was enhanced by deletion of the AR gene. The increase in lesion formation in *ar*-null mice was accompanied by greater accumulation of AGEs. Although STZ-treated mice displayed slightly (20-30%) higher levels of glucose, greater accumulation of AGEs in these mice could not be directly attributed to high glucose alone because deletion of AR increased AGE accumulation

in apoE-null mice without exacerbating hyperglycemia. Furthermore diabetic mice accumulated AGEs that displayed positive reactivity with anti-argpyrimidine, anti-CML as well as anti-3-deoxyglucosone imidazolone antibodies, suggesting that the lack of AR permits greater accumulation of several structurally-diverse AGEs (Fig. 7); consistent with the broad specificity of the enzyme observed in kinetic studies (Table I). Several previous studies, however, suggest that AR is the underlying cause of secondary diabetic complications. This view is based on several decades of work showing that inhibition of AR delays prevents or even reverses cataractogenesis and neuropathy in diabetic rats (42). In addition, it has been recently reported that general overexpression of AR in all tissues exaggerates motor nerve conduction velocity defect (43) and atherosclerosis in diabetic mice (44). However, significance of the effects of such non-specific increase in AR, even in tissues where it is not basally expressed (e.g., smooth muscle cells, liver etc) is not clear. However, our results showing that cardiac specific overexpression of AR increases methylglyoxal and that deletion of AR in the tissues in which it is expressed increases AGE formation and lesion formation in mice indicates that AR promotes the removal of AGE precursors and increases atherosclerotic lesion formation in a tissue-specific manner. It is also likely that the effects of AR may also depend on the state of the disease and the total tissue carbonyl load. Indeed, result from our own laboratory show that inhibition of AR prevents smooth muscle growth and diminishes restenosis in diabetic rats (42) and prevents high glucose-induced inflammatory signaling and the release of TNF-α from vascular smooth muscle cells (45), indicating that inhibition of the enzyme could prevent some of the harmful effects of high glucose. Hence, in different metabolic scenarios, AR may be cytoprotective, by removing toxic aldehydes or harmful because it depletes NADPH and thereby reduces the concentration of reducing equivalents. In this regard, AR may be similar to NF-κB or ROS, both of which are regulated by AR, and both of which could have protective or deleterious effects depending upon the metabolic context. Further studies are required to fully understand the metabolic dependence of AR action. Nevertheless, the data presented here provide direct support to the notion that reduction of methylglyoxal and related AGE precursors is a significant metabolic activity that could be ascribed to AR and that chronic deficiency of this enzyme could increase AGE accumulation and the formation of atherosclerotic lesions.

ACKNOWLEDGEMENTS

This work was supported in part by NIH grants HL 65618, HL55477, HL59378, and RR024489. Technical assistance by Dan Riggs, David Young, Erica Werkman and Barbara Bishop is gratefully acknowledged.

REFERENCES

1. Brownlee,M: Advanced protein glycosylation in diabetes and aging. *Annu Rev Med* 46:223-234, 1995

2. Singh,R, Barden,A, Mori,T, Beilin,L: Advanced glycation end-products: a review. *Diabetologia* 44:129-146, 2001

3. Horie,K, Miyata,T, Maeda,K, Miyata,S, Sugiyama,S, Sakai,H, van Ypersole de,SC, Monnier,VM, Witztum,JL, Kurokawa,K: Immunohistochemical colocalization of glycoxidation products and lipid peroxidation products in diabetic renal glomerular lesions. Implication for glycoxidative stress in the pathogenesis of diabetic nephropathy. *J Clin Invest* 100:2995-3004, 1997

4. Schleicher,ED, Wagner,E, Nerlich,AG: Increased accumulation of the glycoxidation product N(epsilon)-(carboxymethyl)lysine in human tissues in diabetes and aging. *J Clin Invest* 99:457-468, 1997

5. Hammes,HP, Weiss,A, Hess,S, Araki,N, Horiuchi,S, Brownlee,M, Preissner,KT: Modification of vitronectin by advanced glycation alters functional properties in vitro and in the diabetic retina. *Lab Invest* 75:325-338, 1996

6. Schmidt,AM, Hori,O, Chen,JX, Li,JF, Crandall,J, Zhang,J, Cao,R, Yan,SD, Brett,J, Stern,D: Advanced glycation endproducts interacting with their endothelial receptor induce expression of vascular cell adhesion molecule-1 (VCAM-1) in cultured human endothelial cells and in mice. A potential mechanism for the accelerated vasculopathy of diabetes. *J Clin Invest* 96:1395-1403, 1995

7. Wautier,JL, Schmidt,AM: Protein glycation: a firm link to endothelial cell dysfunction. *Circ Res* 95:233-238, 2004

8. Yan,SF, Ramasamy,R, Naka,Y, Schmidt,AM: Glycation, inflammation, and RAGE: a scaffold for the macrovascular complications of diabetes and beyond. *Circ Res* 93:1159-1169, 2003

9. Park,L, Raman,KG, Lee,KJ, Lu,Y, Ferran,LJ, Jr., Chow,WS, Stern,D, Schmidt,AM: Suppression of accelerated diabetic atherosclerosis by the soluble receptor for advanced glycation endproducts. *Nat Med* 4:1025-1031, 1998

10. Sakaguchi,T, Yan,SF, Yan,SD, Belov,D, Rong,LL, Sousa,M, Andrassy,M, Marso,SP, Duda,S, Arnold,B, Liliensiek,B, Nawroth,PP, Stern,DM, Schmidt,AM, Naka,Y: Central role of RAGE-dependent neointimal expansion in arterial restenosis. *J Clin Invest* 111:959-972, 2003

11. Goova,MT, Li,J, Kislinger,T, Qu,W, Lu,Y, Bucciarelli,LG, Nowygrod,S, Wolf,BM, Caliste,X, Yan,SF, Stern,DM, Schmidt,AM: Blockade of receptor for advanced glycation end-products restores effective wound healing in diabetic mice. *Am J Pathol* 159:513-525, 2001

12. Wendt,TM, Tanji,N, Guo,J, Kislinger,TR, Qu,W, Lu,Y, Bucciarelli,LG, Rong,LL, Moser,B, Markowitz,GS, Stein,G, Bierhaus,A, Liliensiek,B, Arnold,B, Nawroth,PP, Stern,DM, D'Agati,VD, Schmidt,AM: RAGE drives the development of glomerulosclerosis and implicates podocyte activation in the pathogenesis of diabetic nephropathy. *Am J Pathol* 162:1123-1137, 2003

13. Conklin,D, Prough,R, Bhatanagar,A: Aldehyde metabolism in the cardiovascular system. *Mol Biosyst* 3:136-150, 2007

14. Shinohara,M, Thornalley,PJ, Giardino,I, Beisswenger,P, Thorpe,SR, Onorato,J, Brownlee,M: Overexpression of glyoxalase-I in bovine endothelial cells inhibits intracellular

advanced glycation endproduct formation and prevents hyperglycemia-induced increases in macromolecular endocytosis. *J Clin Invest* 101:1142-1147, 1998

15. Thornalley,PJ: Glyoxalase I--structure, function and a critical role in the enzymatic defence against glycation. *Biochem Soc Trans* 31:1343-1348, 2003

16. Vander Jagt,DL, Robinson,B, Taylor,KK, Hunsaker,LA: Reduction of trioses by NADPH-dependent aldo-keto reductases. Aldose reductase, methylglyoxal, and diabetic complications. *J Biol Chem* 267:4364-4369, 1992

17. Wermuth,B: Purification and properties of an NADPH-dependent carbonyl reductase from human brain. Relationship to prostaglandin 9-ketoreductase and xenobiotic ketone reductase. *J Biol Chem* 256:1206-1213, 1981

18. Ko,J, Kim,I, Yoo,S, Min,B, Kim,K, Park,C: Conversion of methylglyoxal to acetol by Escherichia coli aldo-keto reductases. *J Bacteriol* 187:5782-5789, 2005

19. Misra,K, Banerjee,AB, Ray,S, Ray,M: Reduction of methylglyoxal in Escherichia coli K12 by an aldehyde reductase and alcohol dehydrogenase. *Mol Cell Biochem* 156:117-124, 1996

20. Schalkwijk,CG, van,BJ, van der Schors,RC, Uchida,K, Stehouwer,CD, van Hinsbergh,VW: Heat-shock protein 27 is a major methylglyoxal-modified protein in endothelial cells. *FEBS Lett* 580:1565-1570, 2006

21. Feron,VJ, Til,HP, de,VF, Woutersen,RA, Cassee,FR, van Bladeren,PJ: Aldehydes: occurrence, carcinogenic potential, mechanism of action and risk assessment. *Mutat Res* 259:363-385, 1991

22. Ulbricht,RJ, Northup,SJ, Thomas,JA: A review of 5-hydroxymethylfurfural (HMF) in parenteral solutions. *Fundam Appl Toxicol* 4:843-853, 1984

23. Allen,RE, Lo,TW, Thornalley,PJ: A simplified method for the purification of human red blood cell glyoxalase. I. Characteristics, immunoblotting, and inhibitor studies. *J Protein Chem* 12:111-119, 1993

24. Gomes,RA, Sousa,SM, Vicente,MH, Ferreira,AE, Cordeiro,CA, Freire,AP: Protein glycation in Saccharomyces cerevisiae. Argpyrimidine formation and methylglyoxal catabolism. *FEBS J* 272:4521-4531, 2005

25. Ahmed,N, Thornalley,PJ: Advanced glycation endproducts: what is their relevance to diabetic complications? *Diabetes Obes Metab* 9:233-245, 2007

26. Goh,SY, Cooper,ME: Clinical review: The role of advanced glycation end products in progression and complications of diabetes. *J Clin Endocrinol Metab* 93:1143-1152, 2008

27. Goldin,A, Beckman,JA, Schmidt,AM, Creager,MA: Advanced glycation end products: sparking the development of diabetic vascular injury. *Circulation* 114:597-605, 2006

28. Srivastava,SK, Ramana,KV, Bhatnagar,A: Role of aldose reductase and oxidative damage in diabetes and the consequent potential for therapeutic options. *Endocr Rev* 26:380-392, 2005

29. Spite,M, Baba,SP, Ahmed,Y, Barski,OA, Nijhawan,K, Petrash,JM, Bhatnagar,A, Srivastava,S: Substrate specificity and catalytic efficiency of aldo-keto reductases with phospholipid aldehydes. *Biochem J* 405:95-105, 2007

30. Srivastava,S, Watowich,SJ, Petrash,JM, Srivastava,SK, Bhatnagar,A: Structural and kinetic determinants of aldehyde reduction by aldose reductase. *Biochemistry* 38:42-54, 1999

31. Srivastava,S, Spite,M, Trent,JO, West,MB, Ahmed,Y, Bhatnagar,A: Aldose reductase-catalyzed reduction of aldehyde phospholipids. *J Biol Chem* 279:53395-53406, 2004

32. Vander Jagt,DL, Kolb,NS, Vander Jagt,TJ, Chino,J, Martinez,FJ, Hunsaker,LA, Royer,RE: Substrate specificity of human aldose reductase: identification of 4-hydroxynonenal as an endogenous substrate. *Biochim Biophys Acta* 1249:117-126, 1995

33. Vander Jagt,DL, Hunsaker,LA: Methylglyoxal metabolism and diabetic complications: roles of aldose reductase, glyoxalase-I, betaine aldehyde dehydrogenase and 2-oxoaldehyde dehydrogenase. *Chem Biol Interact* 143-144:341-351, 2003
34. Dunlop,M: Aldose reductase and the role of the polyol pathway in diabetic nephropathy. *Kidney International* 58:S-3-S-12, 2000
35. Kaiserova,K, Tang,XL, Srivastava,S, Bhatnagar,A: Role of nitric oxide in regulating aldose reductase activation in the ischemic heart. *J Biol Chem* 283:9101-9112, 2008
36. Shinmura,K, Bolli,R, Liu,SQ, Tang,XL, Kodani,E, Xuan,YT, Srivastava,S, Bhatnagar,A: Aldose reductase is an obligatory mediator of the late phase of ischemic preconditioning. *Circ Res* 91:240-246, 2002
37. Niwa,T, Tsukushi,S: 3-deoxyglucosone and AGEs in uremic complications: inactivation of glutathione peroxidase by 3-deoxyglucosone. *Kidney Int Suppl* 78:S37-S41, 2001
38. Szwergold,BS, Kappler,F, Brown,TR: Identification of fructose 3-phosphate in the lens of diabetic rats. *Science* 247:451-454, 1990
39. Hamada,Y, Araki,N, Koh,N, Nakamura,J, Horiuchi,S, Hotta,N: Rapid formation of advanced glycation end products by intermediate metabolites of glycolytic pathway and polyol pathway. *Biochem Biophys Res Commun* 228:539-543, 1996
40. Lal,S, Szwergold,BS, Kappler,F, Brown,T: Detection of fructose-3-phosphokinase activity in intact mammalian lenses by 31P NMR spectroscopy. *J Biol Chem* 268:7763-7767, 1993
41. Ramana,KV, Friedrich,B, Tammali,R, West,MB, Bhatnagar,A, Srivastava,SK: Requirement of aldose reductase for the hyperglycemic activation of protein kinase C and formation of diacylglycerol in vascular smooth muscle cells. *Diabetes* 54:818-829, 2005
42. Srivastava,S, Ramana,KV, Tammali,R, Srivastava,SK, Bhatnagar,A: Contribution of aldose reductase to diabetic hyperproliferation of vascular smooth muscle cells. *Diabetes* 55:901-910, 2006
43. Yagihashi,S, Yamagishi,SI, Wada,RR, Baba,M, Hohman,TC, Yabe-Nishimura,C, Kokai,Y: Neuropathy in diabetic mice overexpressing human aldose reductase and effects of aldose reductase inhibitor. *Brain* 124:2448-2458, 2001
44. Vikramadithyan,RK, Hu,Y, Noh,HL, Liang,CP, Hallam,K, Tall,AR, Ramasamy,R, Goldberg,IJ: Human aldose reductase expression accelerates diabetic atherosclerosis in transgenic mice. *J Clin Invest* 115:2434-2443, 2005
45. Ramana,KV, Tammali,R, Reddy,AB, Bhatnagar,A, Srivastava,SK: Aldose reductase-regulated tumor necrosis factor-alpha production is essential for high glucose-induced vascular smooth muscle cell growth. *Endocrinology* 148:4371-4384, 2007

FIGURE LEGENDS

Fig. 1: High glucose-induced AGE formation. (**A**) Western analysis of total cell lysates prepared from human umbilical vein endothelial cells (HUVECs) cultured in the presence of normal (NG; 5.5 mM) or high (HG; 30 mM) glucose for 7 days and probed with anti-argpyrimidine antibodies. Western blots from two representative experiments are shown. Inset shows the major immunopositive spot resolved by 2D gel analysis of the cell lysates. The spot, corresponding to a molecular weight of 27 kDa and a pI of 7.83, was identified to be HSP27 by MALDI/MS analysis. **(B)** FACS data obtained from HUVECs cultured in normal (*i, iii*) and high (*ii, iv*) glucose. Extracellular AGEs were detected by labeling the cells with the anti-argpyrimdine antibody and phycoerythrin-conjugated secondary antibody. To detect total (extracellular+intracellular) AGEs, the cells were permeabilized before antibody treatment. Relative mean fluorescence was calculated by subtracting the fluorescence obtained from the isotype-matched antibody control. Group data are presented as mean ± S.E.M. * $P < 0.05$ vs normal glucose (NG); n = 3 - 4.

Fig. 2: Methylglyoxal metabolism in endothelial cells. (**A**) GC/MS analysis of acetol formation in HUVECs. For acetol quantification, $^{13}C_3$-methylglyoxal was synthesized from $^{13}C_3$-acetone and $^{13}C_3$-acetol was prepared by incubating $^{13}C_3$-methylglyoxal with AKR1B1 and 0.15 mM NADPH. **(i)** Natural and $^{13}C_3$ methylglyoxal were derivatized using O-(2,3,4,5,6 pentaflourobenzyl)-hydroxylamine hydrochloride (PFBHA) extracted in hexane and separated by gas chromatography. The 1,2 dioxime methylglyoxal eluted with a retention time of 13.1 min (inset). On MS analysis, the fragmentation pattern of ^{12}C-1,2, dioxime methylglyoxal showed a parent ion with m/z of 462. Ions with *m/z* 432 and 265 represents the loss of NO [M-30] and $OC_7H_3F_5$ [M-197] groups respectively, from 1,2 dioxime methylglyoxal. Corresponding ions with *m/z* 465, 435, and 268 are due to the $^{13}C_3$ methylglyoxal. (**ii)** Acetol was derivatized using PFBHA and *N,O*-bis (trimethylsilyl) trifluoroacetamide with trimethylchlorosilane (BSTFA). Derivatized acetol eluted with a retention time of 7.5 min (inset). Ions with *m/z* 326 and 285 were assigned to TMS-2-oxime acetol suffering a loss of CH_3 [M-15] or C_3H_4O [M-56], respectively. Corresponding ions with *m/z* 329 and 286 are due to $^{13}C_3$-acetol. **(iii)** Acetol formation in HUVECs, cultured in media containing 1 mM methylglyoxal for 24 h in the absence and presence of the AKR1B inhibitors sorbinil (50 μM) or tolrestat (25 μM). After treatment, $^{13}C_3$-acetol was added to cell lysates and lysates were derivatized and analyzed by GC/MS. (B) Western analysis of lysates prepared from HUVECs cultured in normal (NG) or high (HG) glucose, with or without sorbinil (50 μM), probed with anti-argpyrimidine and anti-HSP27 antibodies. Intensity of immunopositive band (argpyrimidine) was normalized to HSP27. Data are presented as mean ± S.E.M. $^{*}P < 0.05$ vs cells cultured in the presence of methylglyoxal alone (control) or NG (n = 4) and $^{\#}P < 0.05$ vs HG without sorbinil (n = 4).

Fig. 3: AKR-catalyzed reduction of methylglyoxal in mouse heart: (A) Acetol generated in effluents of isolated WT (C57) or AR-TG hearts perfused with 20 μM methylglyoxal. Acetol concentration was measured by GC/MS following derivatization with PFBHA and BSTFA. $^{13}C_3$ Acetol was used as an internal standard. Data are presented as mean ± S.E.M. * $P < 0.01$ versus WT (n = 4). **(B)** Western analysis of cardiac myocytes isolated from adult male C57 mice probed with antibodies raised against AKR1B1 (AR), AKR1B8 (FR-1) and AKR1A4 (ALDR). Figure shows bands from 3 different mice. **(C)** Rate of methylglyoxal reduction in homogenates prepared from hearts of WT mice (n=6), or mice with a cardiac myocyte-specific transgene expressing AKR1B4 (rat AR; n=6) or AKR1B8 (FR-1; n=6). The enzyme activity was determined with 1 mM methylglyoxal, and 0.15 mM NADPH, with or without 1 μM sorbinil.

Inset shows Western blots from WT and TG hearts developed with anti-AR and anti-FR-1 antibodies. *P<0.01 vs WT (control), #P<0.01 vs AR-TG (control) and § P<0.01 vs FR1-TG (control).

Fig. 4: Genetic ablation of AKR1B3 (AR) diminishes the reduction of AGE precursors. (A) Rate of reduction of glyceraldehyde (**i**), methylglyoxal (**ii**), 3-deoxyglucosone (**iii**), and glyoxal (**iv**), in cardiac homogenates prepared from WT and *akr1b3*-null mice. The enzyme activity was determined with glyceraldehyde (10 mM), glyoxal (1 mM), methylglyoxal (1 mM) or deoxyglucosone (1 mM), and 0.15 mM NADPH, with or without 1 μM sorbinil. Values are presented as mean ± S.E.M. * P < 0.05 versus WT (n = 6). Inset shows the expression of the proteins in WT and AR-KO mice. **(B)** Rate of formation of S-D lactoylglutathione (**i**) and S glycolylglutathione (**ii**) in homogenates prepared from WT and *akr1b3*-null hearts. Glyoxalase I activity was measured with methylglyoxal (1 mM) or glyoxal (1 mM) and GSH (1 mM) in the absence or presence of glyoxalase I inhibitor BBGC (0.2 mM). Inset to panel (**i**) shows Western blots developed from WT and *akr1b3*-null (KO) hearts using the anti-glyoxalase-I antibody. Data are mean ± SEM (n=6). *P<0.01 vs WT (methylglyoxal or glyoxal) and # P<0.01 vs AR-null (methylglyoxal or glyoxal). Inset shows the expression of glyoxalase 1 in WT and AR-KO mice**. (C)** Computer simulations for the relative contributions of AR and glyoxalase I in the metabolism of glyoxal (**i**) and methylglyoxal (**ii**). Relative contribution of the enzymes was calculated on the basis of measurement of AR and glyoxalase I enzyme activities assuming that the concentration of AGE precursors is in steady-state achieved between the processes of formation and those of elimination.

Fig. 5: Increased accumulation of plasma AGEs in the AR-null mice. Western blots of plasma from non-diabetic and diabetic wild type (WT) and *akr1b3*-null (AR-null) mice, probed with anti-argpyrimidine (**A**) and anti-CML (**B**) antibodies. Inset shows positive recognition of glyoxlyic acid treated bovine serum albumin (BSA). Bar graphs show the intensity of indicated anti-argpyrimidine or anti-CML positive bands normalized to Amido-Black stained blots. Data are presented as mean ± S.E.M. *P<0.01 vs WT (control), # P<0.01 vs AR-null (control) and § P<0.01 vs WT diabetic plasma.

Fig. 6: Increased AGE accumulation in the hearts of AR-null mice. (**A**) Western blots of hearts homogenates from diabetic and non-diabetic WT and AR-null mice were probed with anti-argpyrimidine (A) and anti-CML (B) antibodies. Non-diabetic WT and AR-null hearts served as respective controls. The expression of AR, FR-1 and ALDR in the hearts of these mice was examined by the Western blots developed using anti-AR, FR-1 and ALDR antibodies from cardiac homogenates. Recombinant proteins (RP) were used as positive controls. Bar graphs show the intensity of the indicated anti-argpyrimidine or anti-CML positive bands normalized to GAPDH. Data are presented as mean ± S.E.M. *P < 0.01 vs WT control, # P<0.01 vs AR-null (control) and § P<0.01 vs WT diabetic. (**C**) Immuno histochemical analyses of AGE accumulation in hearts of diabetic WT and AR-null mice. Sections were stained with anti-argpyrimidine antibody and staining was quantified by image analysis. Group data shows the extent of staining quantified using the MetaMorph imaging software. Data are presented as mean ± S.E.M. * P<0.01 vs WT (diabetic).

Fig. 7: Genetic ablation of AR exacerbates diabetic lesion formation and AGE accumulation. (**A**) Photomicrographs of cross sections of innominate arteries of 20 week old non diabetic (control) and diabetic *apoE*-null and *apoE/akr1b3*-null mice. Sections were stained with hematoxylin and eosin, and the lesion area was quantified by image analysis. Data are presented as mean ± S.E.M. *P < 0.01 versus *apoE*-null (control), # P<0.01 vs AR/*apoE*-null

(control) and § P<0.01 vs *apoE*-null (diabetic). Arterial sections of diabetic *apoE*-null and *apoE/akr1b3*-null mice stained with anti-argpyrimidine (**B**), anti-CML (**C**) and anti-3deoxyglucosone-imidazolone (**D**) antibodies. The extent of staining was quantified by image analysis. Data are presented as mean ± S.E.M. *P < 0.05 vs *apoE*-null (diabetic).

Table 1: *Steady state kinetic parameters for the reduction of AGE precursors by AKRs.*

Substrates	**Gen bank accession number**	**Proteins**	**K_m (µM)**	**k_{cat}(min^{-1})**	**k_{cat}/K_m ($min^{-1}µM^{-1}$)**
Glyoxal	NM_021473	AKR1A4	3229±904	45.8±4.2	0.014
	NM_001628	AKR1B1	350±20	29.5±2.02	0.082
	NM_009658	AKR1B3	333±62	12.1±0.36	0.036
	NM_009731	AKR1B7	7450±1500	5.6±0.35	0.001
	NM_008012	AKR1B8	635±81	20±0.52	0.031
	NM_020299	AKR1B10	7800±359	8.87±0.63	0.002
	NM_030611	AKR1C3	NDA	-	-
	NM_013778	AKR1C6	12073±1031	12.8±0.67	0.001
	NM_134066	AKR1C18	NDA	-	-
	NM_025337	AKR7A5	5931±1393	12.87±0.27	0.002
Methylglyoxal		AKR1A4	874±91	483±0.27	0.55
		AKR1B1	22±2	37.2±2.21	1.698
		AKR1B3	35±4	19.5±2.3	0.56
		AKR1B7	1996±274	8.9±0.31	0.004
		AKR1B8	184±15	18.2±1.21	0.098
		AKR1B10	1250±89	26.82±5	0.389
		AKR1C3	NDA	-	-
		AKR1C6	139±35	7.65±0.7	0.054
		AKR1C18	NDA	-	-
		AKR7A5	9075±1250	22±0.7	0.002
Furfural		AKR1A4	5918±1379	17.4±0.78	0.002
		AKR1B1	316±34	30.86±1.91	0.097
		AKR1B3	69±10	13.36±0.93	1.91
		AKR1B7	NDA	-	-
		AKR1B8	622±100	2.6±0.27	0.001
		AKR1B10	1617±287	178±15	0.11
		AKR1C3	156±35	3.09±0.33	0.019
Hydroxymethyl Furfural		AKR1A4	6428±1479	24.05±4	0.003
		AKR1B1	482±92	14.55±2	0.03
		AKR1B3	98±15	4.15±0.3	0.042
		AKR1B7	NDA	-	-
		AKR1B8	1197±117	7.82±0.05	0.016
		AKR1B10	1117±135	100±15	0.085
		AKR1C3	1939±425	167±0.02	0.008
Deoxyglucosone		AKR1A4	2067±178	777±25	0.376
		AKR1B1	112±5	38.9±2	0.345
		AKR1B3	89±5	11.6±1	0.13
		AKR1B10	3293±118	14.36±1.9	0.004
		AKR1B10	3293±118	14.36±1.9	0.004

Enzyme activity was measured in 0.1 M potassium phosphate (pH 7.0) using the indicated substrates and 0.15 mM NADPH at room temperature. Proteins were reduced with DTT prior to assay. NDA, no detectable activity.

Fig. 1

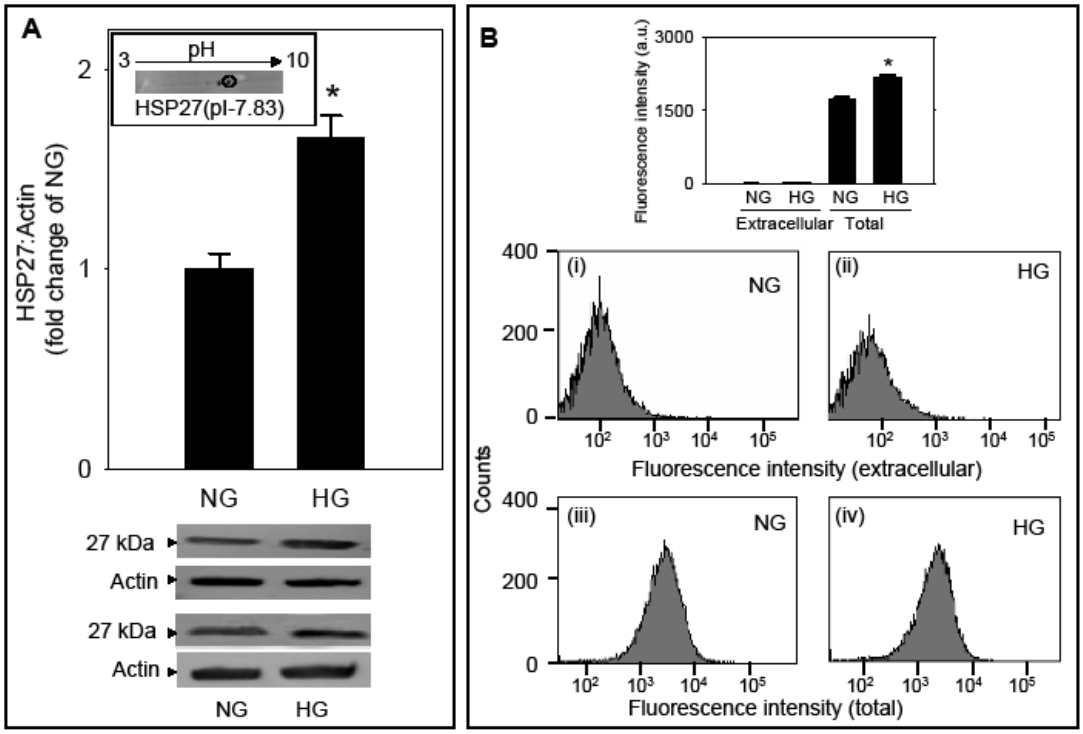
A
pH
3
10
HSP27(pI-7.83)
HSP27:Actin
(fold change of NG)
NG
HG
27 kDa
Actin
B
Fluorescence intensity (a.u.)
Extracellular
Total
(i)
(ii)
(iii)
(iv)
Counts
Fluorescence intensity (extracellular)
Fluorescence intensity (total)

Fig. 2

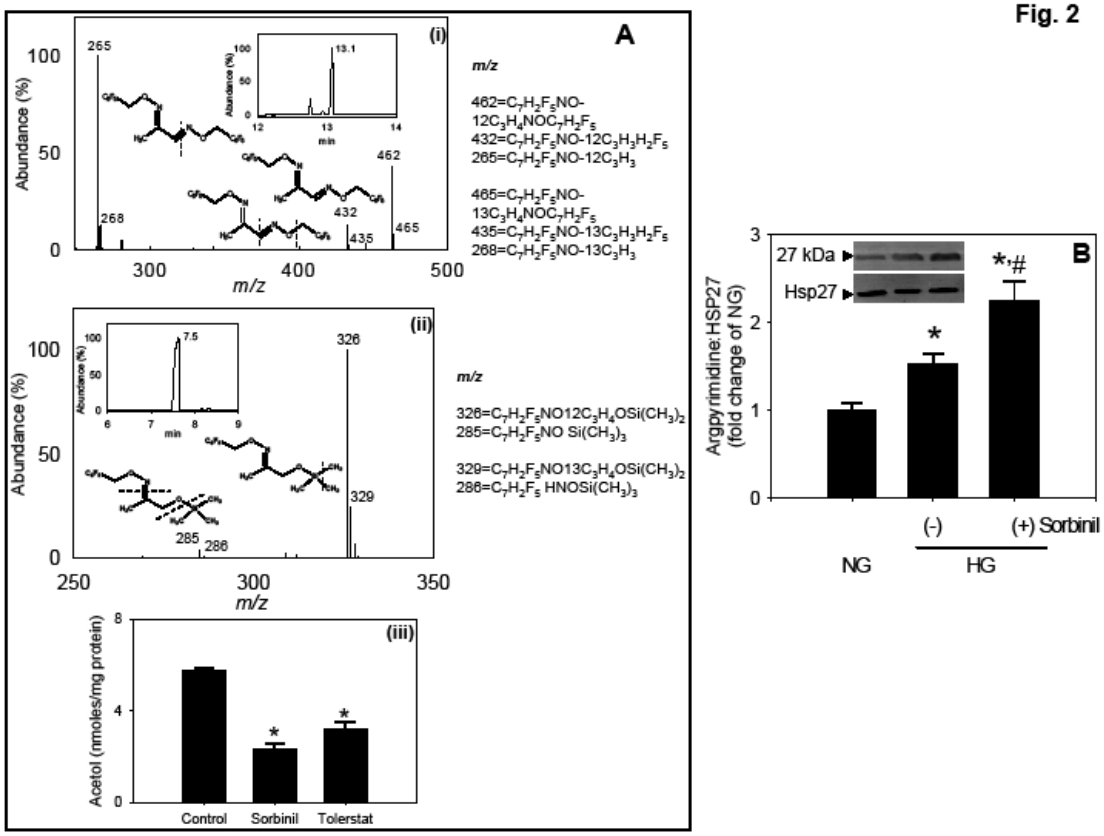
A
(i)
(ii)
(iii)
Abundance (%)
m/z
462=C7H2F5NO-12C3H4NOC7H2F5
432=C7H2F5NO-12C3H3H2F5
265=C7H2F5NO-12C3H3
465=C7H2F5NO-13C3H4NOC7H2F5
435=C7H2F5NO-13C3H3H2F5
268=C7H2F5NO-13C3H3
326=C7H2F5NO12C3H4OSi(CH3)2
285=C7H2F5NO Si(CH3)3
329=C7H2F5NO13C3H4OSi(CH3)2
286=C7H2F5 HNOSi(CH3)3
Acetol (nmoles/mg protein)
Control
Sorbinil
Tolerstat
B
27 kDa
Hsp27
Argpyrimidine:HSP27
(fold change of NG)
(-)
(+) Sorbinil
NG
HG

Fig. 3

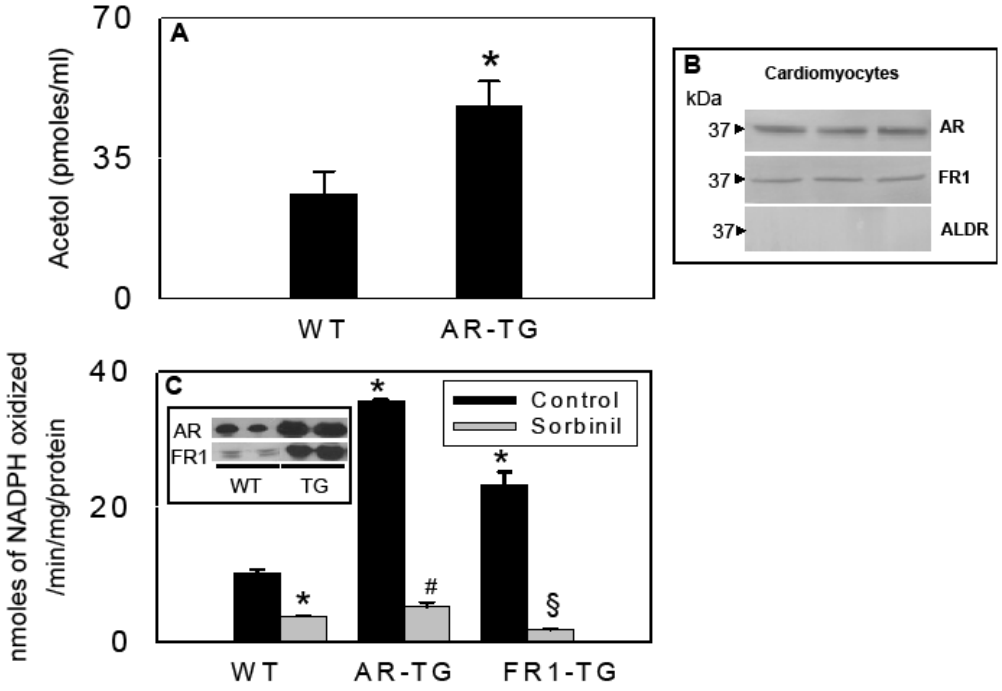
A
Acetol (pmoles/ml)
70
35
0
WT
AR-TG
B
Cardiomyocytes
kDa
37
AR
FR1
ALDR
C
nmoles of NADPH oxidized /min/mg/protein
40
20
0
Control
Sorbinil
AR
FR1
WT
TG
WT
AR-TG
FR1-TG

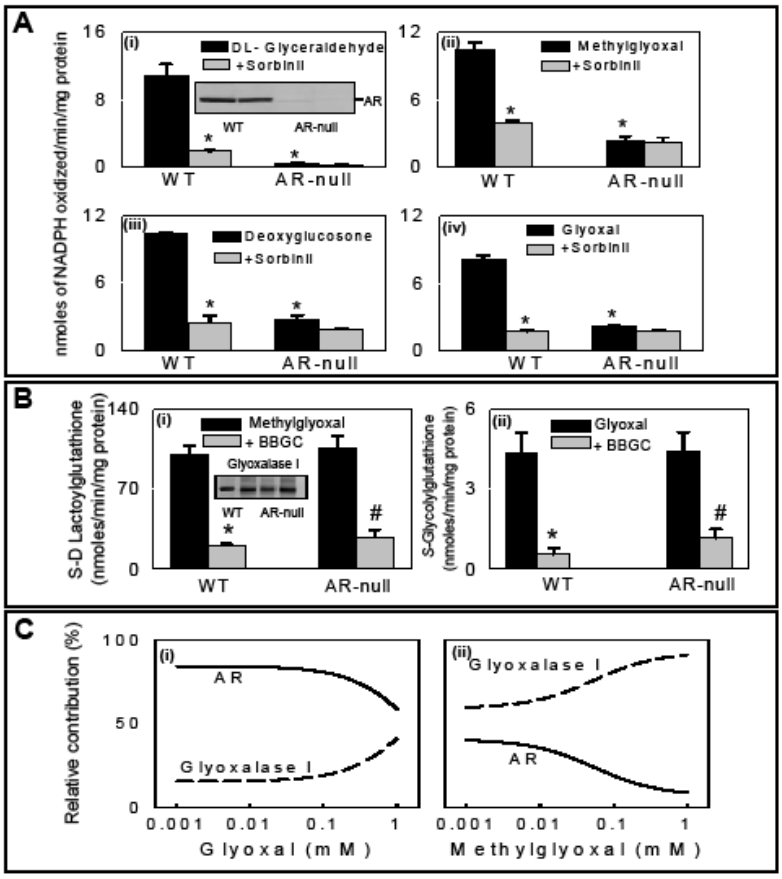
A
nmoles of NADPH oxidized/min/mg protein
(i) DL- Glyceraldehyde
+Sorbinil
AR
WT
AR-null
(ii) Methylglyoxal
(iii) Deoxyglucosone
(iv) Glyoxal
B
S-D Lactoylglutathione (nmoles/min/mg protein)
(i) Methylglyoxal
+ BBGC
Glyoxalase I
S-Glycolylglutathione (nmoles/min/mg protein)
(ii) Glyoxal
C
Relative contribution (%)
100
50
0
(i) AR
Glyoxalase I
(ii) Glyoxalase I
AR
0.001
0.01
0.1
1
Glyoxal (mM)
Methylglyoxal (mM)

Fig. 4

Fig. 5

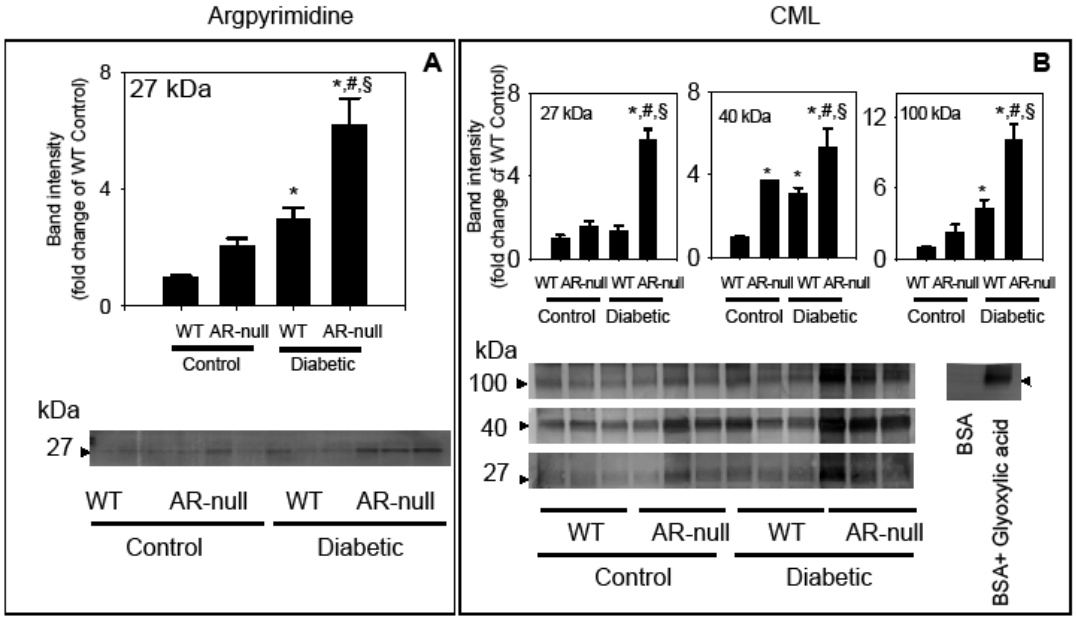
Argpyrimidine
CML
A
B
27 kDa
40 kDa
100 kDa
Band intensity (fold change of WT Control)
*,#,§
WT AR-null WT AR-null
Control Diabetic
kDa
100
40
27
BSA
BSA+ Glyoxylic acid

Fig.6

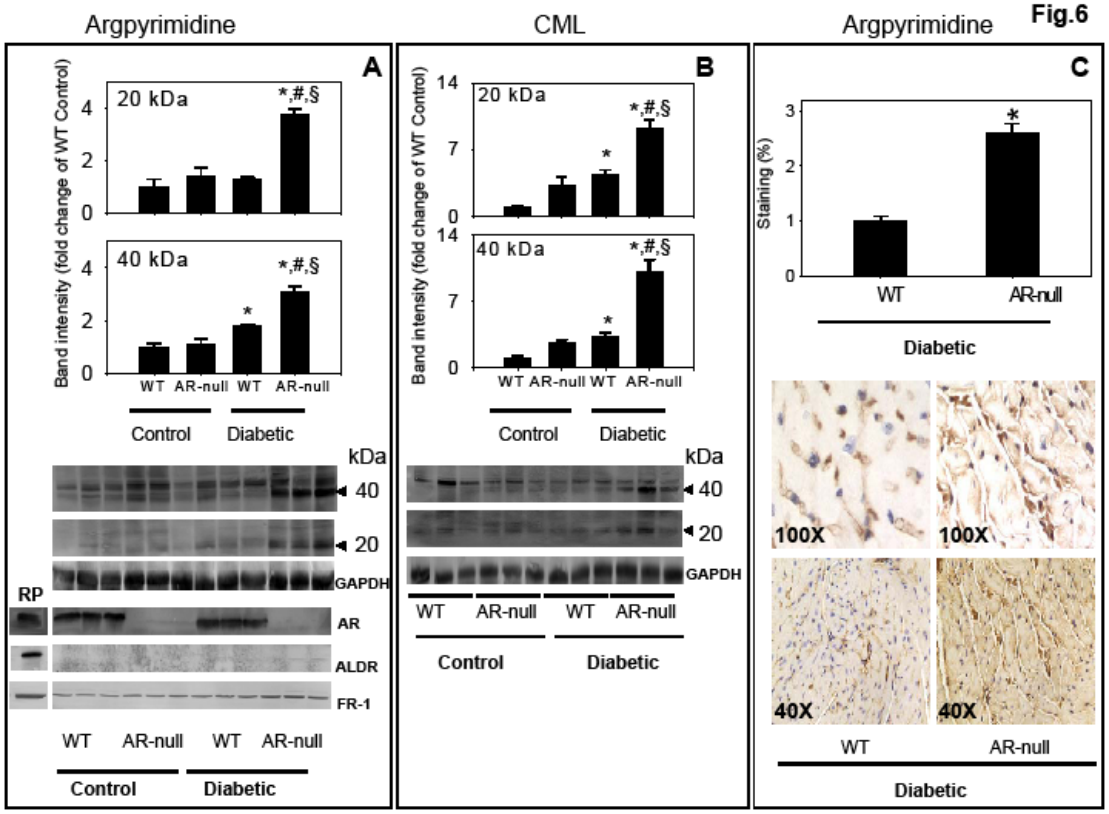
Argpyrimidine
CML
Argpyrimidine
A
B
C
20 kDa
40 kDa
Band intensity (fold change of WT Control)
Staining (%)
kDa
40
20
GAPDH
RP
AR
ALDR
FR-1
WT AR-null WT AR-null
Control Diabetic
WT AR-null
Diabetic
100X
40X

Fig. 7

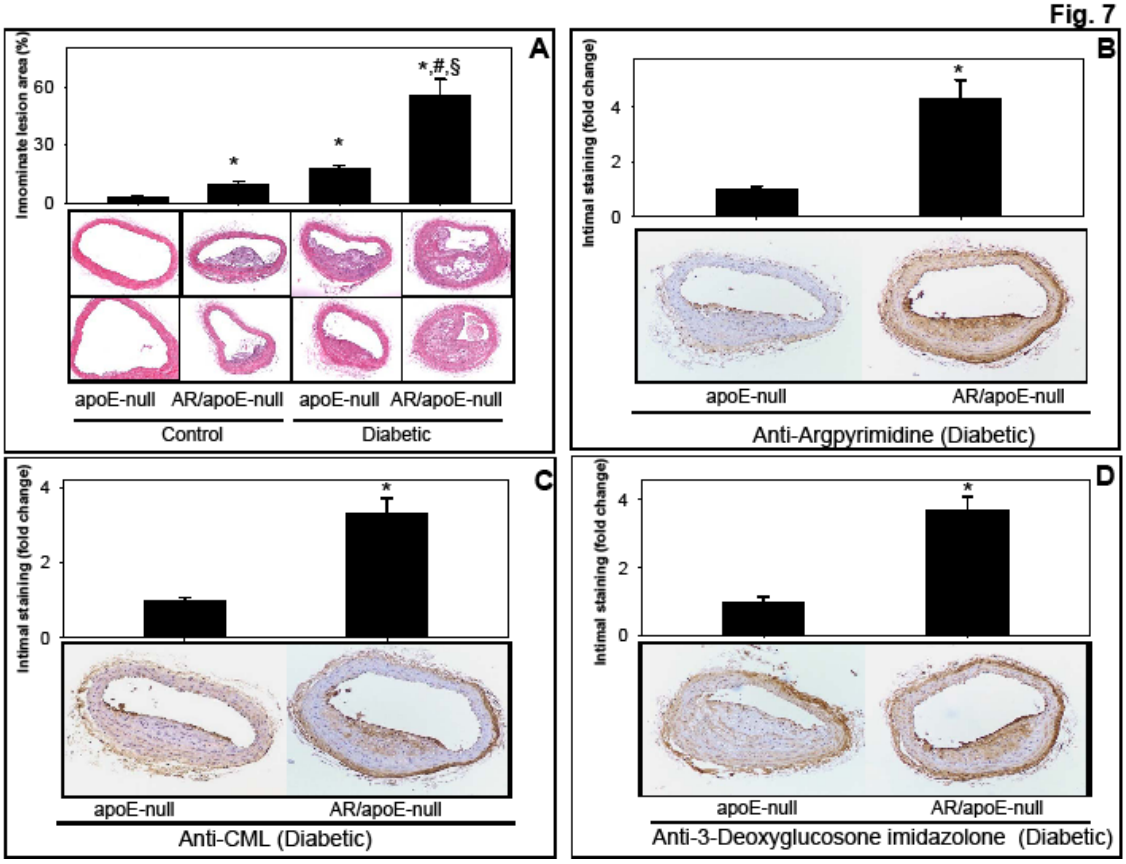
A
Innominate lesion area (%)
60
30
0
*
*
*,#,§
apoE-null
AR/apoE-null
apoE-null
AR/apoE-null
Control
Diabetic
B
Intimal staining (fold change)
4
2
0
*
apoE-null
AR/apoE-null
Anti-Argpyrimidine (Diabetic)
C
Intimal staining (fold change)
4
2
0
*
apoE-null
AR/apoE-null
Anti-CML (Diabetic)
D
Intimal staining (fold change)
4
2
0
*
apoE-null
AR/apoE-null
Anti-3-Deoxyglucosone imidazolone (Diabetic)